First-Principles Study of Electron-Conduction Properties of C_{60} Bridges

Tomoya Ono and Kikuji Hirose

Department of Precision Science and Technology, Osaka University, Suita, Osaka 565-0871, Japan

(Received 20 June 2006; published 11 January 2007)

The electron-conduction properties of fullerene-based nanostructures suspended between electrodes are examined by first-principles calculations based on the density functional theory. The electron conductivity of the C_{60}-dimer bridge is low owing to the constraint of the junction of the molecules. When the fullerenes are doped electrons by being inserted Li atoms into the cages, the unoccupied state around the junction is filled and the conductivity can be significantly improved.

DOI: 10.1103/PhysRevLett.98.026804 PACS numbers: 73.40.−c, 71.15.−m, 72.80.Rj, 85.65.+h

Since the first report on the fullerene structure of C_{60}, extensive research has been devoted to understanding the electronic structures of fullerene-based nanostructures [1] because of their interesting physical properties such as superconductivity and magnetism. In a benchmark study toward understanding the electron-conduction properties of fullerenes, C_{60} molecules have the possibility of being a nanoscale electrical amplifier using a scanning tunneling microscope tip [2]. Palacios *et al.* also reported that a single C_{60} bridge, in which a fullerene is sandwiched between electrodes, exhibits metallic properties and that its conductance is between $1G_0$ and $3G_0$ [3]. In analogy with graphite intercalated compounds, injection of electron and hole carriers into fullerenes is expected for the cases of alkali and halogen dopings, respectively [4]. One example is the endohedral fullerenes which encapsulate metal atoms inside their cages in formation process using arc-discharge vaporization of composite rods made of graphite and metal oxide [5]. At present stage, because of the abundance of C_{60} in the usual fullerene production, fullerene-based materials have more practical importance owing to their possibilities for novel components in miniaturized electronic devices and a reliable study should be performed to obtain the information.

In this Letter, we examined the electron-conduction properties of C_{60} molecules suspended between semi-infinite gold electrodes using first-principles calculations within the framework of the density functional theory [6]. Our results indicate that the conductance of the C_{60} dimer is $\sim 0.1G_0$ owing to the scattering of incident electrons at the junction between the molecules, whereas that of the C_{60} monomer is $\sim 1G_0$. By encapsulating Li atoms in their cages, the dimer exhibits good conductivity. The energy of the unoccupied molecular orbitals at the junction shifts down to the Fermi level, and as a consequence, the conductance of the Li@C_{60} dimer significantly increases. To explore the doping mechanism of the C_{60} bridges, we also compared the energy band structures of the infinite C_{60}, Li@C_{60}, and Li chains and found that the Li@C_{60} chain is a conductor due to the electron transfer from the Li atom to the fullerene, while the other chains are insulators.

Our first-principles calculation method for electron-conduction properties is based on the real-space finite-difference approach [7–9]. The norm-conserving pseudopotentials [10] of Troullier and Martins [11] are employed to describe the electron-ion interaction, and exchange correlation effects are treated by the local density approximation [12]. We employ the computational model in which the C_{60} molecule is sandwiched between electrodes [see, for example, Fig. 4(c)]. Because polymerized C_{60} was found to form a parallel double-bonded structure in the previous study [13], a model in which a C_{60} molecule is connected to electrodes with parallel double bonds is employed. Since many first-principles investigations using structureless jellium electrodes are in almost quantitative agreement with experiments, we substitute the jellium electrodes for crystal ones [14,15]. To determine the optimized atomic structures and Kohn-Sham effective potential, a conventional supercell is employed under the periodic boundary condition in all directions; the size of the supercell is $L_x = L_y = 30.8$ a.u. and $L_z = L_{\mathrm{mol}} + 25$ a.u., where L_x and L_y are the lateral lengths of the supercell in the x and y directions parallel to the electrode surfaces, respectively, L_z is the length in the z direction, and L_{mol} is the length of the inserted molecules. The C_{60} monomers and dimers are put between the electrodes. The structural optimizations are implemented in advance with a real-space grid spacing of ~ 0.33 a.u. The molecules are optimized individually under the isolated condition and then relaxed between the electrodes. Although the initial distance between the edge atoms of inserted molecules and the Au(111) atom plane in the jellium electrode is set at 3.20 a.u., this distance increases after the structural optimization of the molecules with the jellium electrodes. For the conductance calculation, we take a grid spacing of ~ 0.50 a.u. The Kohn-Sham effective potential is computed using the supercell employed in the structural optimization. We ensured that the increase in the cutoff energy and the enlargement of the supercell did not affect our conclusion significantly. The scattering wave functions from the left electrode are written as

 © 2007 The American Physical Society

$$\Psi_i^L = \begin{cases} \Phi_i^{\text{in}} + \sum_j r_{ij}^L \Phi_j^{\text{ref}} & \text{(in the left electrode)}, \\ \phi_i^L & \text{(in the scattering region)}, \\ \sum_j t_{ij}^L \Phi_j^{\text{tra}} & \text{(in the right electrode)}, \end{cases}$$

where Φ's are the bulk wave functions inside the electrodes. The reflection coefficients r^L, transmission coefficients t^L, and the wave function in the scattering region ϕ^L are evaluated by the overbridging boundary-matching formula [8,9] under the nonperiodic condition in the z direction. The conductance of the nanowire system at the limits of zero temperature and zero bias is described by the Landauer-Büttiker formula, $G = \mathrm{Tr}(\mathbf{T}^\dagger\mathbf{T})G_0$ [16], where $\mathbf{T}$ is the transmission matrix. To investigate states actually contributing to electron conduction, the eigenchannels are computed by diagonalizing the Hermitian matrix $\mathbf{T}^\dagger\mathbf{T}$ [15].

We first calculate the electron-conduction properties of the C_{60} monomer. Figure 1(a) shows the total charge and current distributions of the scattering wave functions Ψ^L. The current distribution is derived by the equation of continuity. The electron currents pass along the C-C bonds, and not directly cross through the inside of the C_{60} cages. The charge distributions of the lowest unoccupied molecular orbitals (LUMOs) of the isolated C_{60} monomer are shown in Fig. 1(b). The C_{60} has three t_{u1} degenerate LUMOs and we name, for convenience, the states that are odd functions with respect to the y-z, z-x and x-y planes as $t_{u1,x}$, $t_{u1,y}$, and $t_{u1,z}$, respectively. The incident electrons are found to be scattered at both interfaces between the molecule and the electrodes. The channel transmissions of the respective states are collected in the first column of Table I. It can be seen that the $t_{u1,z}$ state dominantly contributes to electron conduction. According to the wave-function matching formula for the three-dimensional jellium wire [17], the transmission of the channel that has high kinetic energy in the direction parallel to the bridge is large and is hardly affected by the length of the wire. The transmission of the $t_{u1,z}$ state is higher than those of the other degenerate t_{u1} states, since its kinetic energy in the z direction is the largest. The resultant conductance is $1.13G_0$, which is in agreement with the previous theoretical calculations, which report that the C_{60} monomer exhibits metallic electron-conduction properties and that its conductance is between $1G_0$ and $3G_0$ [3].

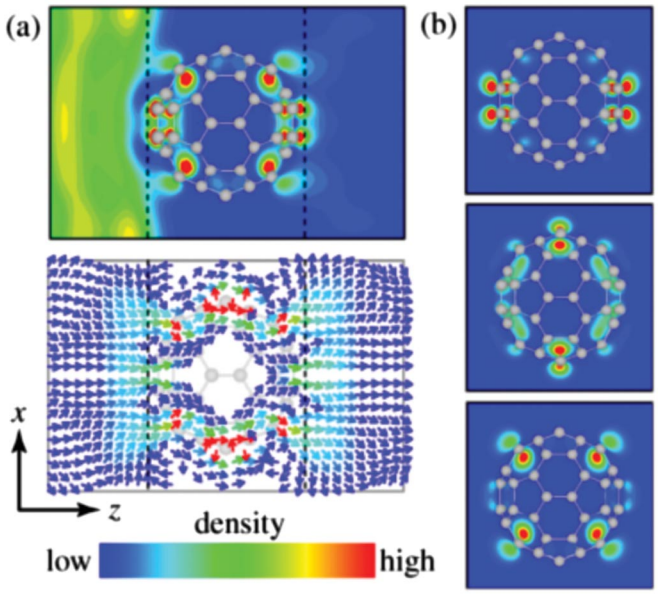

FIG. 1 (color). [(a), top] Total charge distribution of scattering wave functions Ψ^L at the Fermi level when C_{60} is suspended between electrodes. [(a), bottom] Total current distribution. The planes shown are perpendicular to the electrode surfaces and contain the atoms facing the electrodes. (b) Charge distributions of three degenerate LUMOs of isolated C_{60} molecule for $t_{u1,x}$ (top), $t_{u1,y}$ (middle) and $t_{u1,z}$ (bottom). The spheres, lines, and vertical dashed lines represent carbon atoms, C-C bonds, and the edges of the jellium electrodes, respectively. The magnitude of the charge and current densities is represented according to the color bar. In (a), the maximum (minimum) range of the color bar is $3.70(0.0) \times 10^{-3}$ e/eV bohr^3 for the charge distribution and $1.14(0.23) \times 10^{-9}$ A/V bohr^2 for the current distribution.

Next, the conduction property of the dimer is examined. Figure 2(a) shows the total charge and current distributions. Since the reflection of electrons occurs at the junction in addition to the interfaces, the conductance has a lower value ($0.11G_0$) than that of the C_{60} monomer. This situation is similar to that of C_{20} [18]. The channel transmissions are listed in the second column of Table I. Note that all the channel transmissions are lower than those of C_{60}. In the case of the isolated C_{60} dimer, the characteristics of the first and second LUMOs of the isolated dimer are inherited from the $t_{u1,y}$ and $t_{u1,z}$ LUMOs of the isolated C_{60} molecule, respectively. The contribution of the second LUMO to electron conduction is the largest, although its energy is higher than that of the first LUMO. According to our result, the conductances of the longer bridges are expected to decay rapidly as the number of fullerenes in the bridges increases because of their nonmetallic properties. Do fullerene-based bridges never work as conductive molecule wires?

It has been reported that endohedral metal fullerenes, in which metal atoms are encapsulated in cages, are produced by the collisions of metal ions with C_{60} vapor molecules [5]. Here, Li atoms are inserted into the cages so as to locate on the central axis of the bridge. The total energy gain realized by encapsulating the Li atoms is 3.89 eV per dimer, the cohesive energy of the $(\mathrm{Li@C_{60}})_2$ molecule is

TABLE I. Channel transmissions at the Fermi level.

	C_{60}	$(C_{60})_2$	$(Li@C_{60})_2$
$t_{u1,x}$	0.110	0.001	0.007
$t_{u1,y}$	0.133	0.012	0.020
$t_{u1,z}$	0.873	0.098	0.851

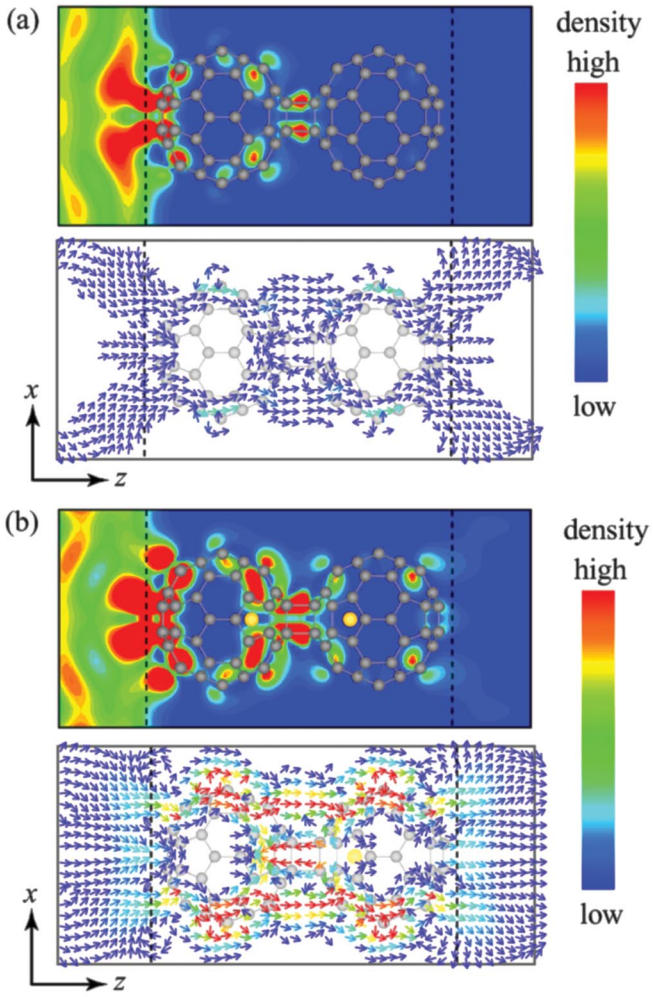

FIG. 2 (color). [(a), top] Total charge distribution of scattering wave functions Ψ^L at the Fermi level. [(a), bottom] Total current distribution. The planes shown, the meanings of the symbols, and the range of the color bars are the same as those in Fig. 1. (b) Similar to (a) but for $(Li@C_{60})_2$. The yellow spheres are Li atoms.

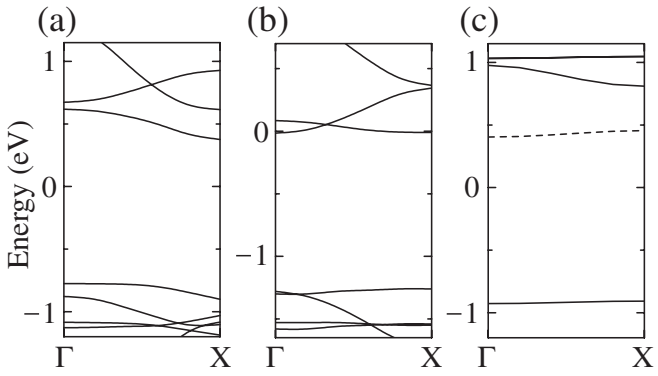

FIG. 3. Energy band structures of (a) pure fullerene chain, (b) endohedral fullerene chain, and (c) Li chain with infinite length. The band structure is shown in a supercell containing one C_{60} molecule or one Li atom. The length of the supercell is 17.19 a.u. and the zero of energy is set to be the Fermi level. The Li atom is placed at the center of the cage in the case of endohedral chain. The solid and dashed curves in (c) represent majority and minority spins, respectively.

0.10 eV per $Li@C_{60}$ molecule, and the energy difference between the highest occupied molecular orbital and LUMO is 0.21 eV, which is markedly smaller than that of $(C_{60})_2$ (1.33 eV). We show in Fig. 2(b) the total charge and current distributions of the $(Li@C_{60})_2$ molecule. The reflection at the junction of the molecules is suppressed and the conductance reaches $0.88G_0$. We show the channel transmissions in the third column of Table I. The transmissions of the states consisting of the $t_{u1,z}$ orbital are significantly larger than those of $(C_{60})_2$ and recover up to that of the monomer.

The energy band structures of the infinite chains are depicted in Fig. 3. The $Li@C_{60}$ chain exhibits metallic property, while the others are nonmetallic. Moreover, the Li chain is spin polarized whereas the others are paramagnetic, and the states originating from the Li chain disappear in the $Li@C_{60}$ chain. In addition, although each band shifts, the band structure of the $Li@C_{60}$ chain is not significantly deformed from that of the C_{60} chain. Thus, injection of electrons into the fullerenes can be achieved by inserting atoms into the cages. However, the Fermi level of the molecules attached to electrodes can shift due to the electrons transfer to/from the electrodes of electrons, which is relevant to the electron affinities of inserted atoms and electrodes, and the unpaired electrons of endohedral fullerenes form covalent bonds. Therefore, the dimer remains an insulator if the Fermi level exists inside the gap. Figure 4 shows the density of states (DOS) of the $(C_{60})_2$ and $(Li@C_{60})_2$ suspended between the electrodes, which are plotted by integrating the DOS on the plane perpendicular to the bridges. The inserted Li atoms do not largely affect the DOS at the interface between the dimer and electrodes. Yet, around the junction of the molecules, the states that are ~0.3 eV above the Fermi level of the C_{60} dimer is shifted down to the Fermi level by being inserted the Li atoms, which makes the unoccupied state of the junction filled. The doping of the fullerenes plays a prominent role rather than the rehybridizations of the bonds of the fullerenes, since even the $(Li@C_{60})_2$ without relaxing the geometry upon insertion possesses a high conductivity $(0.95G_0)$. Therefore, the endohedral fullerene bridge is expected to be a good conductor even when the molecules are a bit deformed by phonons or mechanical stress from the electrode [2].

In conclusion, we have theoretically investigated the electron-conduction properties of C_{60} bridges. The C_{60} dimer does not possess good conductivity, because the junction of the molecules is a bottleneck of electron conduction. On the other hand, by encapsulating the Li atoms into the cages, the C_{60} dimer exhibits good conduction properties due to the shift of the LUMO at the junction. These results indicate that the endohedral metal fullerene

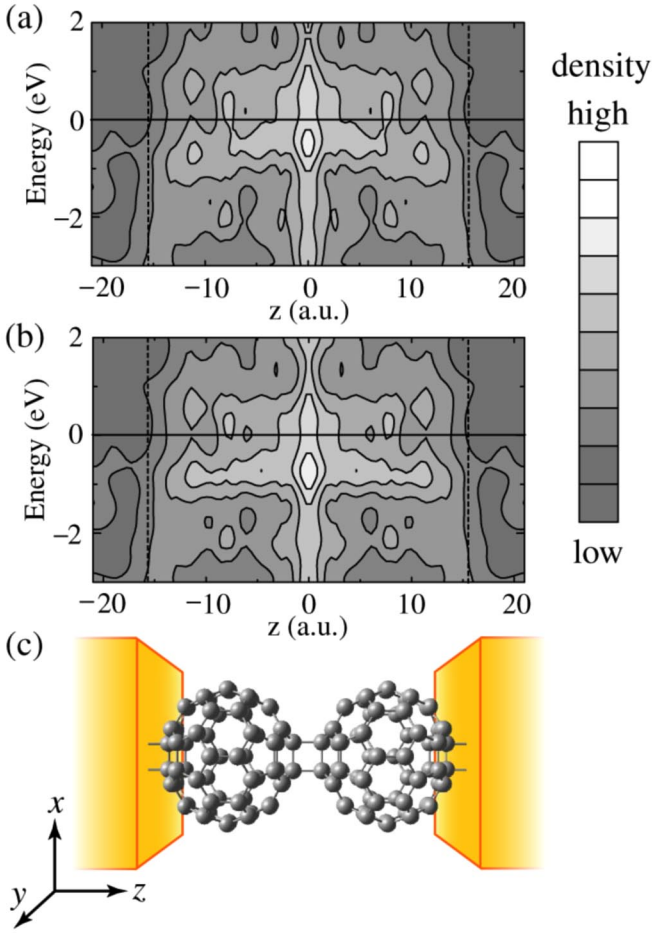

FIG. 4 (color online). Distributions of DOS integrated on plane perpendicular to bridge as functions of relative energy from the Fermi level for (a) $(C_{60})_2$ bridge and (b) $(Li@C_{60})_2$ bridge. The zero of energy is chosen to be the Fermi level. Each contour represents twice or half the density of adjacent contour lines and the lowest contour is 1.47×10^{-5} e/eV bohr. The vertical dashed lines represent the edge of the jellium electrodes. A schematic diagram of the computational model for the C_{60} dimer is illustrated in (c) as a visual aid.

bridges have potential applications in electronic devices. In addition, encapsulating metal atoms into fullerene will be a novel scheme of controlling the electron-conduction properties of the fullerene bridges. Thus, this situation will stimulate a new technology of electronic devices using molecule bridges.

This research was partially supported by a Grant-in-Aid for the 21st Century COE "Center for Atomistic Fabrication Technology," by a Grant-in-Aid for Scientific Research in Priority Areas "Development of New Quantum Simulators and Quantum Design" (Grant No. 17064012) from the Ministry of Education, Culture, Sports, Science and Technology. The numerical calculation was carried out by the computer facilities at the Institute for Solid State Physics at the University of Tokyo and the Information Synergy Center at Tohoku University.

[1] See, for example, S. Saito and A. Oshiyama, Phys. Rev. Lett. **66**, 2637 (1991); N. Hamada, S. I. Sawada, and A. Oshiyama, *ibid.* **68**, 1579 (1992); K. Ohno *et al.*, *ibid.* **76**, 3590 (1996); S. Okada, S. Saito, and A. Oshiyama, *ibid.* **83**, 1986 (1999); E. Burgos *et al.*, *ibid.* **85**, 2328 (2000); M. Saito and Y. Miyamoto, *ibid.* **87**, 035503 (2001), and Refs. [2,3,5,18].

[2] C. Joachim and J. K. Gimzewski, Chem. Phys. Lett. **265**, 353 (1997).

[3] J. J. Palacios, A. J. Perez-Jimenez, E. Louis, and J. A. Verges, Phys. Rev. B **64**, 115411 (2001).

[4] Y. Miyamoto, A. Rubio, X. Blase, M. L. Cohen, and S. G. Louie, Phys. Rev. Lett. **74**, 2993 (1995); G. Csányi *et al.*, Nature Phys. **1**, 42 (2005).

[5] Z. Wan, J. F. Christian, and S. L. Anderson, Phys. Rev. Lett. **69**, 1352 (1992).

[6] P. Hohenberg and W. Kohn, Phys. Rev. **136**, B864 (1964).

[7] J. R. Chelikowsky, N. Troullier, and Y. Saad, Phys. Rev. Lett. **72**, 1240 (1994); T. Hoshi, M. Arai, and T. Fujiwara, Phys. Rev. B **52**, R5459 (1995); A. P. Seitsonen, M. J. Puska, and R. M. Nieminen, *ibid.* **51**, 14 057 (1995); J.-L. Fattebert and J. Bernholc, *ibid.* **62**, 1713 (2000); G. F. Bertsch, J. I. Iwata, A. Rubio, and K. Yabana, *ibid.* **62**, 7998 (2000); P. A. Khomyakov and G. Brocks, *ibid.* **70**, 195402 (2004); J. J. Mortensen, L. B. Hansen, and K. W. Jacobsen, *ibid.* **71**, 035109 (2005); T. L. Beck, Rev. Mod. Phys. **72**, 1041 (2000).

[8] K. Hirose, T. Ono, Y. Fujimoto, and S. Tsukamoto, *First-Principles Calculations in Real-Space Formalism, Electronic Configurations and Transport Properties of Nanostructures* (Imperial College Press, London, 2005).

[9] T. Ono and K. Hirose, Phys. Rev. Lett. **82**, 5016 (1999); Phys. Rev. B **72**, 085105 (2005); **72**, 085115 (2005); K. Hirose and T. Ono, *ibid.* **64**, 085105 (2001); Y. Fujimoto and K. Hirose, *ibid.* **67**, 195315 (2003).

[10] We used the norm-conserving pseudopotentials NCPS97 constructed by K. Kobayashi. See K. Kobayashi, Comput. Mater. Sci. **14**, 72 (1999).

[11] N. Troullier and J. L. Martins, Phys. Rev. B **43**, 1993 (1991).

[12] J. P. Perdew and A. Zunger, Phys. Rev. B **23**, 5048 (1981).

[13] P. Zhou, Z.-H. Dong, A. M. Rao, and P. C. Eklund, Chem. Phys. Lett. **211**, 337 (1993).

[14] N. D. Lang, Phys. Rev. B **55**, 4113 (1997); M. Okamoto and K. Takayanagi, *ibid.* **60**, 7808 (1999); S. Tsukamoto and K. Hirose, *ibid.* **66**, 161402(R) (2002); N. D. Lang and M. Di Ventra, *ibid.* **68**, 157301 (2003); S. Okano, K. Shiraishi, and A. Oshiyama, *ibid.* **69**, 045401 (2004).

[15] N. Kobayashi, M. Brandbyge, and M. Tsukada, Phys. Rev. B **62**, 8430 (2000).

[16] M. Buttiker, Y. Imry, R. Landauer, and S. Pinhas, Phys. Rev. B **31**, 6207 (1985).

[17] Y. Egami, T. Ono, and K. Hirose, Phys. Rev. B **72**, 125318 (2005).

[18] M. Otani, T. Ono, and K. Hirose, Phys. Rev. B **69**, 121408(R) (2004).